A portable rotating disc as blood rheometer

Cite as: Biomicrofluidics **13**, 064120 (2019); https://doi.org/10.1063/1.5128937
Submitted: 23 September 2019 . Accepted: 19 November 2019 . Published Online: 02 December 2019

Rahul Agarwal, Arnab Sarkar, Subhechchha Paul, and Suman Chakraborty

A portable rotating disc as blood rheometer

Cite as: Biomicrofluidics 13, 064120 (2019); doi: 10.1063/1.5128937
Submitted: 23 September 2019 · Accepted: 19 November 2019 ·
Published Online: 2 December 2019

Rahul Agarwal,[1] Arnab Sarkar,[2,3] Subhechchha Paul,[4] and Suman Chakraborty[1,a)]

AFFILIATIONS

[1]Department of Mechanical Engineering, Indian Institute of Technology Kharagpur, Kharagpur 721302, India
[2]Department of Mechanical Engineering, Indian Institute of Technology (BHU) Varanasi, Varanasi 221005, India
[3]School of Medical Science and Technology, Indian Institute of Technology Kharagpur, Kharagpur 721302, India
[4]Department of Mechanical Engineering, Indian Institute of Engineering Science and Technology, Shibpur 711103, India

[a)]**Author to whom correspondence should be addressed:** suman@mech.iitkgp.ernet.in, **Tel.:** +91-3222-282990.

ABSTRACT

Abnormalities in biophysical properties of blood are often strong indicators of life threatening infections. However, there is no existing device that integrates the sensing of blood hematocrit (or equivalently, packed cell volume), viscosity, and erythrocyte sedimentation rate (ESR) in a unified paradigm for point-of-care diagnostics. In an effort to develop a rapid, integrated, accurate, portable, and inexpensive sensing platform to diagnose the corresponding pathophysical parameters, we develop a simple and portable spinning disk capable of yielding these results in a few minutes instead of the traditional duration of hours. The device requires only 40 μl of unprocessed freshly drawn blood treated with an anticoagulant ethylenediaminetetraacetic acid, instead of the traditional requirement of 2 ml of blood for just the ESR measurement and still more for hematocrit determination. In contrast to the sophisticated instrumentation required to determine these parameters by the previously proposed microfluidic devices, our device requires minimal infrastructure. The measurement of hematocrit is accomplished by means of a simple 15 cm ruler. Additionally, a simple measurement of the blood flow rate enables the determination of the ESR value. The rapidity, ease, accuracy, portability, frugality, and possible automation of the overall measurement process of some of the most important parameters of blood under infection pinpoint its utility in extreme point-of-care settings.

I. INTRODUCTION

Microfluidic devices are highly efficient miniaturized platforms for fluid manipulation that offer economy of the reagent and sample, low cost, low energy fluid propulsion, lower operational times, and most importantly, environment friendly disposal.[1–9] Their most important applications lie as point-of-care (POC) biomedical devices in resource-limited settings.[10,11] Various devices[12] have been proposed for applications like malaria detection,[13] smart painless needle,[14] oral drug delivery,[15] sepsis diagnosis,[16] detection of circulating tumor DNA,[17] and for determining general blood characteristics.[18] The microfluidic technologies have different manifestations like paper based capillary microfluidics[19–21] often controlled by a smartphone,[22] flexible wearable sensors,[23] and centrifugal microfluidics,[12,24–26] among many others.[27–29] Of these, centrifugal microfluidics have gained prominence owing to myriad possibilities of fluid manipulation[30–36] like a Coriolis force based flow switch[37] and utilization of the Coriolis effect as a diagnostic marker.[38] Simultaneous actuation of the multiple flow process by a simple act of rotation[39–41] has made it an attractive option for POC medical devices.[42–44] Some of the notable examples include cellular lysis, detection of food borne pathogens,[5,6] dengue detection,[45] DNA extraction, blood plasma separation,[46,47] and whole blood testing,[3,48–50] among others.[51,52]

Erythrocyte sedimentation rate (ESR), the blood hematocrit level, and blood viscosity are some of the most important blood parameters that indicate the state of infection and beyond.[53,54] The settling of red blood cells (RBCs), known as erythrocyte sedimentation rate,[55] has been long used for the detection of acute inflammatory infections,[56,57] rheumatic and coronary heart diseases,[58] pregnancy,[59] and several other pathological conditions.[60] It is also significant for studying *in-vitro* flow dynamics,[61] *in-vivo* flow properties, and resistance to the blood flow.[62] It is generally measured in millimeters per hour with the normal range being 0–22 mm/h for men and 0–29 mm/h for women. An abnormally high value of ESR is an indication of the occurrence of a disease, and hence, ESR becomes a common diagnostic test. Since the rouleaux formation tendency is largely affected by the fibrinogen level in plasma,[63] a measure of ESR is also indicative of the plasma

protein levels. The most commonly employed traditional methods for ESR determination are the Westergren method and the Wintrobe method.[64] In these methods, undiluted blood samples are anticoagulated with K_3EDTA using glass pipets, and sedimentation due to gravity is allowed. During sedimentation, the pipets are mounted vertically on supporting racks at room temperature. The time taken for this sedimentation is 1–2 h, and accordingly, ESR is measured after 1 h and subsequently after 2 h. Some of the newer methods utilize bioelectrical impedance.[65] These methods are time consuming, are laborious, and require bulk consumption of blood. Consequently, the focus shifted to microfluidic platforms[66] for estimation of various hematological properties. Various methods were proposed like the periodic measurement of ESR in parallel microfluidic channels.[67] These methods, however, failed to lower the complexity level of the overall fabrication process.

Along with ESR, the blood hematocrit level and viscosity are two other important parameters that greatly affect blood dynamics throughout the circulatory system.[68] From the perspective of hyperviscosity syndrome and cardiovascular diseases, it is important to measure plasma and serum viscosity. Various macroscale viscometers have been reviewed in the past.[69] Electrical impedance technique,[70] reversal flow switching in a microfluidic channel,[71] a physiometer,[72] and several other microfluidics based systems[73–76] have also been proposed. Blood viscosity, in turn, is significantly affected by the hematocrit level of blood. Hematocrit is defined as the volume percentage of red blood cells (RBCs) in a given whole blood volume. Centrifuge driven platforms have been the gold standard for measuring hematocrit. Several microfluidic POC devices[77] have been developed to measure the hematocrit level of blood under different pathological conditions. In dengue fever, monitoring the hematocrit (or equivalently, packed cell volume) is critically important since an abnormal rise in the same may indicate a lethal dehydration in the vital organs as a consequence of the infection or a disorder such as polycythemia vera, whereas an abnormal decrease may indicate anemia or a white blood cell disorder such as leukemia. For the blood hematocrit related parameters, i.e., viscosity and ESR, although portable microfluidics system[78] and other methods like a driving syringe system[79] and a microfluidic-based speckle analysis method[80] delivered the required results, they could not cater to rapid medical diagnostics in resource-limited settings.

The interdependence of the three parameters of blood, hematocrit, viscosity, and ESR, warrants the development of a microfluidic device that could deliver the estimation of all of these simultaneously. In this work, we propose a simple spinning disk that is able to accurately measure the ESR, hematocrit, and blood viscosity with just 40 μl of unprocessed, freshly collected, and anticoagulant ethylenediaminetetraacetic acid (EDTA) treated whole blood. We exploit the rotational physics of a spinning disk to actuate the flow and measure hematocrit by a readily available 15 cm ruler, with a least count of 0.5 mm. We then estimate blood viscosity by employing a power law model and establish the agreement of our predicted power law indices with the standard rheological data obtained from a cone and plate type rheometer. We finally measure the volumetric flow rate of whole blood and utilize the empirical dependence of ESR on hematocrit and the flow rate to estimate ESR with reasonable accuracy in comparison to the gold standard methods. Our results are likely to be of fundamental importance not only in the context of biomedical diagnostics, but also in other application areas addressing transport phenomena over various spatiotemporal scales.[81–92]

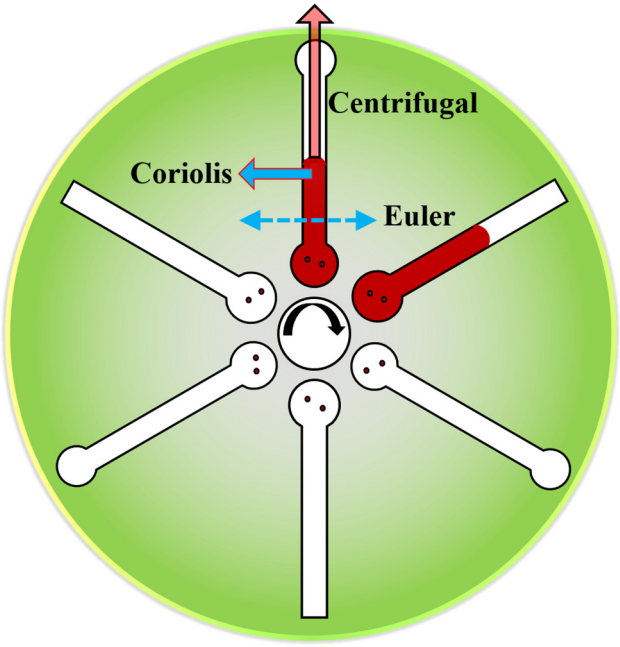

FIG. 1. Schematic illustrating various rotational forces on the blood flow in a microchannel. The various forces are as follows: Centrifugal force, Coriolis force, and the Euler force.

In a rotational reference frame, various forces are generated by the act of rotation. These forces are (Fig. 1): the centrifugal force, the Coriolis force, and the Euler force. The volumetric centrifugal force $F_{cent} = \rho(\vec{\omega} \times (\vec{\omega} \times \vec{r}))$ always acts radially outward. The volumetric Coriolis force $F_{Coriolis} = 2\rho(\vec{\omega} \times \vec{V})$ acts normal to the net flow only when there is a relative motion of the fluid in the rotational reference frame, whereas the volumetric Euler force $F_{Euler} = \rho\left(\frac{d\vec{\omega}}{dt} \times \vec{r}\right)$ acts only when the angular velocity is time varying. In the above expressions, ρ is the density of fluid, $\vec{\omega}$ is the angular velocity of the disk, $\vec{r}$ is the position vector from the origin, $\vec{V}$ is the flow velocity relative to the rotating reference frame, and t is the time. In this work, we utilize the effect of centrifugal force for actuation of the flow in our device. Even though the Coriolis force is very much present in our device, it does not influence the analysis or performance as the flow velocity relative to the rotational reference frame is quite low (~mm/s).

II. MATERIALS AND METHODS

A. Materials and device fabrication

The proposed microfluidic device is a compact disk (CD) made up of three layers: the top layer, the middle layer, and the

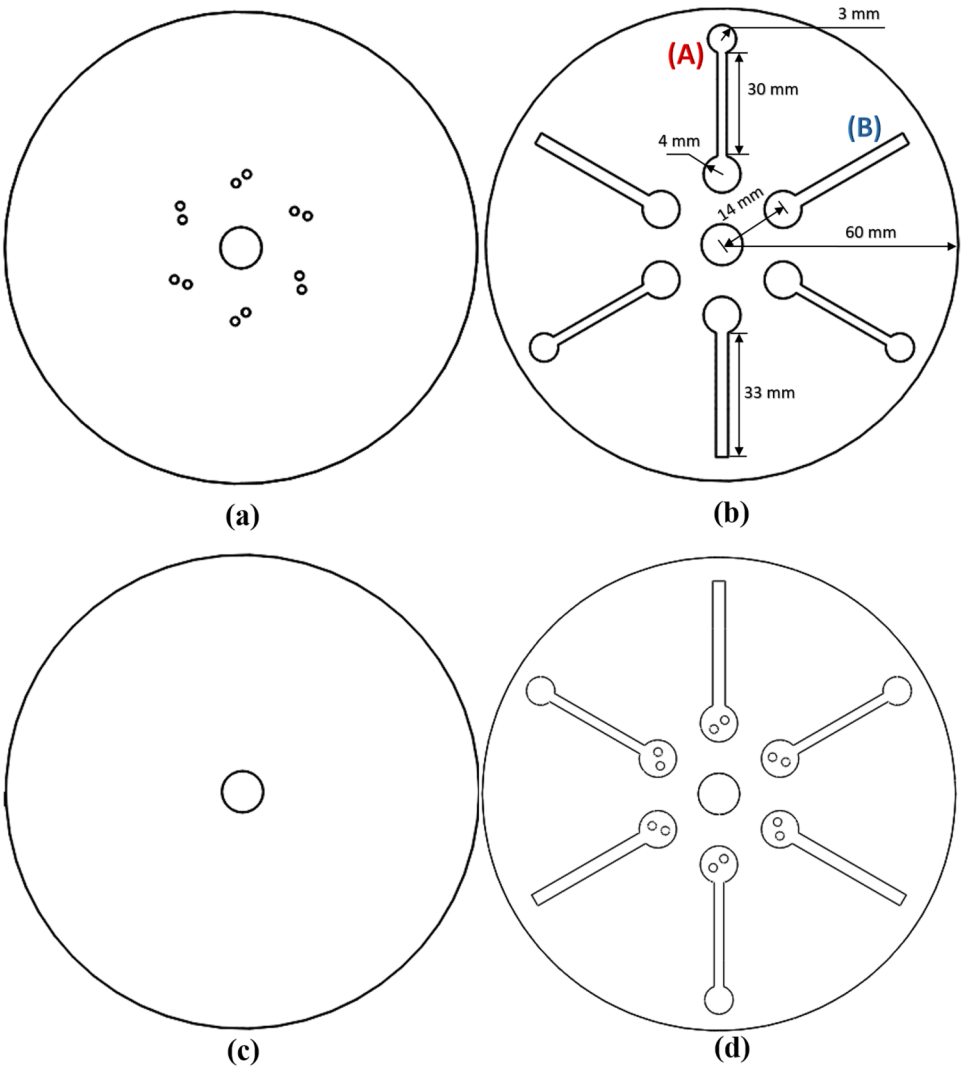

FIG. 2. Disc fabrication process. (a) The top layer of PMMA containing the sample loading and pressure balancing holes. (b) The middle layer of PSA containing the patterns for microfluidic channels. (c) The bottom layer of PMMA forming the base of the microfluidic channels and providing the structural support to the overall disc. (d) Composite spinning disc formed by integrating the top, the middle, and the bottom layers.

bottom layer. The top layer [Fig. 2(a)] is cut out from a 0.4 mm thick polymethyl-methacrylate (PMMA) sheet, and it contains the sample loading and the pressure balancing holes. The middle layer [Fig. 2(b)] is cut out from a 100 μm thick, clear, double sided adhesive tape [pressure sensitive adhesive (PSA)], and it contains the patterns for microfluidic channels. It contains two types of microchannels: type (A) for measuring the flow rate, and type (B) for measuring the blood hematocrit level. The dimensions of both types of microchannels and other features of the disk are indicated in Fig. 2(b). The bottom layer [Fig. 2(c)] is simply a circle cut out from a 1 mm thick PMMA sheet, and its role is to provide structural support to the overall disk while also forming the base of the microfluidic channels. The PMMA sheets are machined by a table top CNC (T-Tech Inc. QC 5000). 1 mm cutting diameter drill bit is used for making sample loading and pressure balancing holes, whereas a carbide router tool of 1.4 mm cutting diameter is used for machining all the other features in the PMMA sheet. An adhesive cutter/plotter (Graphtec CE 6000-60 Plus) is used for patterning microfluidic channels in the middle adhesive layer. Eventually, all the three layers are aligned together to form the composite compact disk structure [Fig. 2(d)], which is then passed through a mechanical roller press to seal the microfluidic channels against any leakages under centrifugal force.

B. Channel design

There are two types of channels: type (A) and type (B). Both types of channels are 100 μm in height (as dictated by the thickness of PSA). Width of both the channels is 3 mm. Although it could be argued that the type (A) channel is similar to Kar *et al.*[93] and the type (B) channel is similar to Riegger *et al.*,[94] the key differences lie in the fact that both the reported channels have

widths of ~500 μm and have other features like a slope,[94] etc. Not only this, the loading and the pressure balancing holes are spatially separated, and there is a possibility of fluid spillage due to wobbling of the disk, i.e., out of plane vibrations. The proposed designs eliminate both of these issues as follows: first, by designing the loading and the pressure balancing holes close together (to eliminate the possibility of fluid spillage), and second, by designing the channels having width of the order of millimeters (3 mm to be precise). This not only simplifies the fabrication process as micromachining is now not required to carve out the patterns for the channels, as this is done by simply cutting the PSA (accomplished by means of a blade in the vinyl cutter). Ideally, one would be able to fabricate the disk without utilizing any sophisticated machining equipment as the PMMA sheet does not have any complex features. The micronature of the channel is accomplished by utilizing the PSA of 100 μm thickness.

C. Sample collection and processing

All the blood samples were collected from the in-house Hospital of the parent Institute of the corresponding author, following appropriate Ethical clearance from the Institutional Ethical Committee. The samples were drawn from veins (i.e., venous blood) as it is commonly utilized for routine pathological evaluations. The collected samples were stored in a tube precoated with ethylenediaminetetraacetate at 4 °C. The samples were collected on multiple days and without any bias. From the collected samples, different samples were selected for experimental runs such that the entire range of parameters under investigation, i.e., hematocrit and ESR, were covered. Since the investigated blood samples are venous in nature, the proposed device is expected to yield convincing results at least for kiosk based diagnostics. The idea of this type of facility would be to provide a kiosk in a resource poor locality, where people can visit and have their blood based parameters evaluated at extremely low costs and with minimal power consumption. Additionally, this device could also be tested for capillary blood. It is expected that even in the case of capillary blood, the performance of the device will be convincing, the only change being the calibrations. This would then enable its deployment for bedside diagnostics. It must be noted that the healthy and nonhealthy levels of hematocrit are rather subjective and vary with age and sex. Therefore, an attempt is made to cover the physiologically relevant range of hematocrit (~30%–45%) for the experimental investigations. Similarly, ESR values under 30 mm/h are considered to be normal (making allowances for age and sex). We have, therefore, focused on selecting the samples such that both the healthy and nonhealthy ranges of ESR could be covered (~0 mm/h–110 mm/h).

D. Experimental methodology

The disk has six microchannels; three each for the flow rate measurement and the hematocrit measurement. One compact disk essentially provides three observations each for the flow rate and the hematocrit, which are ensemble averaged to account for experimental variability. These 6 observations could be of the same or different samples. After fabricating the disk, it is coupled to an in-house rotational drive. This completes step 1 [Fig. 3(a)]. Then, the blood sample (20 μl) is loaded into each of the two microchannels through the sample loading holes: one for the flow rate measurement and the other for the hematocrit measurement. This completes step 2 [Fig. 3(b)]. We now turn on the rotation at 1150 RPM. This speed is identified as ω_{fl}, speed for the flow rate measurement. This completes step 3 [Fig. 3(c)]. We then measure the time taken for the blood to fill the end reservoir of the type (A) channel by a simple mobile stopwatch. Upon loading the sample, as the blood gradually moves inside the channel, it replaces the air that previously occupied that space. This air exits through the pressure balancing hole. The visualization of the blood reaching the end reservoir is aided by a stroboscope synced to the frequency of the disk. This completes step 4 [Fig. 3(d)]. Although it could be argued that the use of a stroboscope prohibits the utility of this device for POC diagnostics, it must be noted that it does not require a synced camera or an associated computer for its operation. The data collection is manual in nature and is done with the aid of a stopwatch. We then increase the rotational speed to 3000 RPM. This speed is identified as ω_{Ht}, speed for the hematocrit measurement. The rotation is turned off after 5 min. This completes step 5 [Fig. 3(e)]. Finally, in the type (B) channel, the total length of blood (pelleted RBCs column and the plasma column) sample (l_T) and the length of just the pelleted RBCs column (l_R) are measured by a readily available 15 cm ruler having a least count of 0.5 mm. A resolution of 0.5 mm is deemed to be sufficient as, first, the ensemble averaged readings are to be considered and, second, the lengths that are not exactly at 0.5 mm counts are snapped to the nearest 0.5 mm counts. This is not much different than rounding a hematocrit reading obtained by the gold standard technique. While making the measurement of the lengths with the ruler, the disk is placed on a level surface in the same position for different readings. The flatness of the surface is ensured by a spirit level. This ensures that the ruler is well aligned with the channel whose lengths are to be measured. This completes step 6 [Fig. 3(e)]. The ratio of these two lengths is defined as the hematocrit, i.e., $Ht = \frac{l_R}{l_T}$.

E. Rheometer measurements

The rheological data have been collected from a strain controlled cone and plate type rheometer (Anton Paar MCR 302, cone angle 2°, plate diameter 25 mm, and shear rate 10 s^{-1}–500 s^{-1}). For each sample, a set of 3 independent experimental runs has been conducted. For each viscosity vs shear rate curve of a sample, the power law indices are extracted by curve fitting, which are then ensemble averaged to obtain the mean and the standard error.

F. Data analysis

Each point in all the graphs has been ensemble averaged over at least three independent experimental runs. The experimental data are represented as mean ± standard error, unless stated otherwise. These independent runs account for both the variability introduced due to different channels and the variability introduced due to different compact disks. All the data have been collected by a single researcher; therefore, it does not take into account the variability introduced due to different users. However, the simplicity of the process is expected to shield the collected data from user errors.

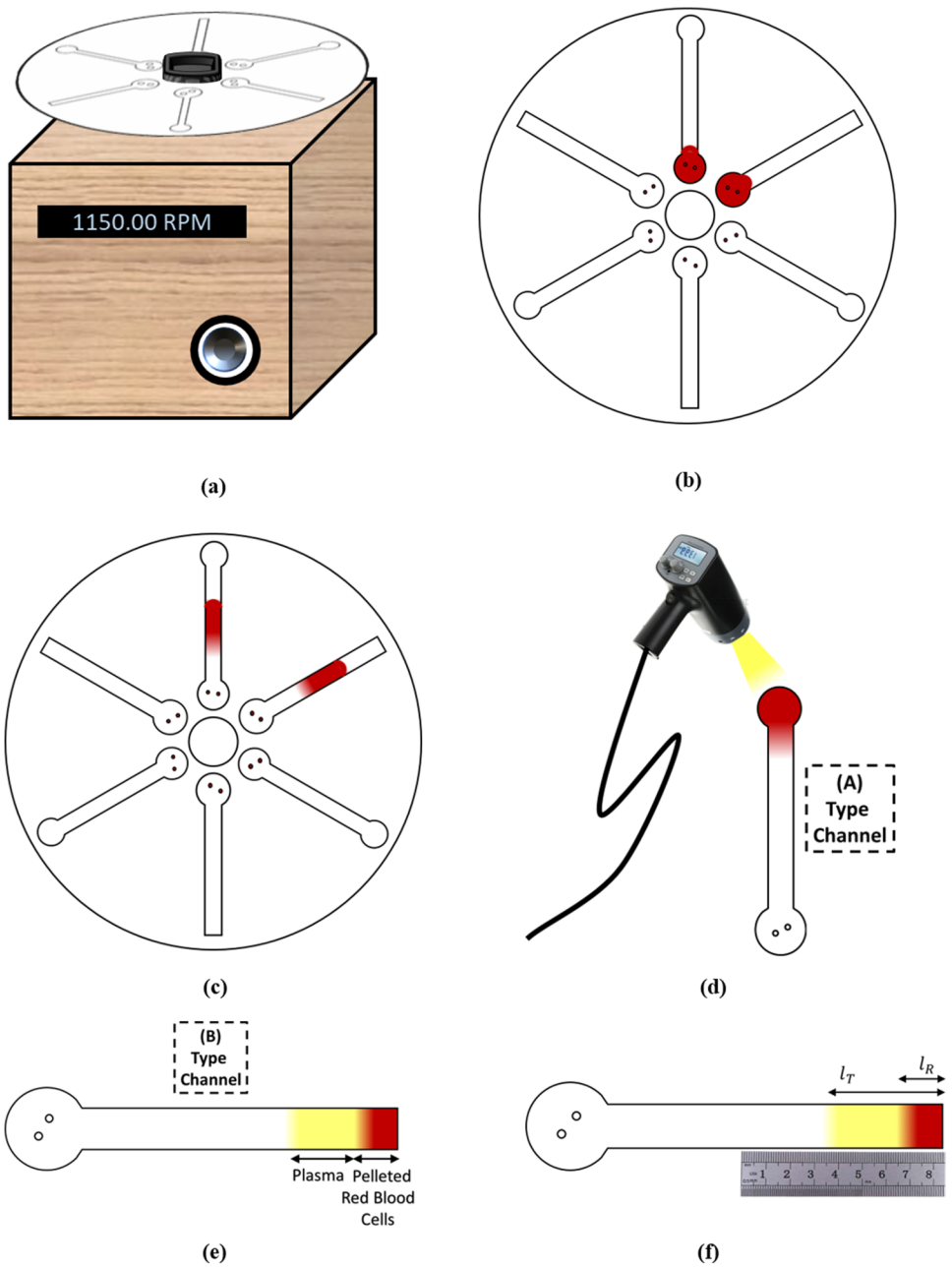

FIG. 3. Complete experimental execution scheme. (a) Coupling of the disc to the rotational drive (step 1). (b) Loading of the blood sample in each of the type (A) and type (B) channels (step 2). (c) Rotation turned on at 1150 RPM (step 3). (d) Measurement of time for the blood to completely fill the end reservoir of the type (A) channel. Visualization is aided by a stroboscope synced with the speed of the rotational drive (step 4). (e) Increase the rotational speed to 3000 RPM and allow the rotation for 5 min (step 5). (f) Measure the lengths of the column of the pelleted RBCs, and the total length comprising the plasma and the pelleted RBCs (step 6).

All the data analyses, i.e., algebraic calculations and calibrations, were done in MATLAB and MS Excel.

III. RESULTS AND DISCUSSION

A. Calculation of the burst frequency

Burst frequency is defined as the rotational frequency above which the centrifugal force overcomes the surface tension effects and initiates the flow. It is given as[25]

$$f_b = \sqrt{\frac{\sigma \cos(\theta) C}{4A(\Delta R)\bar{R}\rho\pi^2}}, \tag{1}$$

where σ is the surface tension coefficient, θ is the contact angle, C is the wetted perimeter, A is the area of the cross section, ΔR is the radial length of the fluid column in the reservoir, and $\bar{R}$ is the space

TABLE I. Typical property values.

Surface tension coefficient (σ)	0.072 N/m
Contact angle (θ)	20°
Wetted perimeter (C)	6.2 mm
Cross-section area (A)	0.3 mm^2
Length of the fluid column in reservoir (ΔR)	8 mm
Position of the fluid column in reservoir ($\bar{R}$)	14 mm
Density of blood (ρ)	1060 kg/m^3

averaged position of the fluid column in the reservoir. The property values are given in Table I. Upon inserting the required values in Eq. (1), we get $f_b \sim 17.3$ Hz ~ 1050 RPM. Please note that this burst frequency is the same for both the types of channels: type (A) and type (B) [Fig. 2(b)] since the inlet geometries and the radial locations are the same for both of them.

B. Hematocrit measurement

Blood hematocrit is defined as the volume percentage of the RBCs in a given sample of whole blood. Upon high speed centrifugation, blood separates into its different constituents based on their densities. Since centrifugal force is a space dependent body force ($F_{cent} = \rho\omega^2 r$), its magnitude increases as we go further away from the axis of rotation. It is also noteworthy that the centrifugal force will be much larger on a heavier substance than on a relatively lighter substance. Therefore, due to centrifugation, RBCs being the heaviest settle at the outermost region of the microchannel, whereas this region is followed by other cellular components and then the plasma. Hence, once the whole blood reaches the end of a closed channel, the centrifugation then leads to the initiation of separation of blood into its different constituents based on density difference. Upon allowing centrifugation at $\omega_{Ht} = 3000$ RPM for sufficiently long time, a steady state in terms of separation of components is attained. This sufficiently long time is rather subjective and was decided to be 5 min after repeated trials for different durations revealed that after 5 min, there was no measurable change in the lengths of the columns of plasma and pelleted RBCs. Now, since the cross-sectional area of the microchannel is constant throughout (once the inlet region is crossed), the ratio of the length of the column occupied by only the pelleted RBCs (l_R) and the separated plasma plus the pelleted RBCs (l_T) will indicate the volume percentage of the RBCs in that blood sample, i.e., $Ht = \frac{l_R}{l_T}$. Quite significantly, this measurement will be independent of the channel width and depth, as long as the channel cross-sectional area is the same throughout the volume of the separated blood. The experimental results are depicted in Fig. 4. An excellent agreement ($R^2 = 0.99$) of the hematocrit level is observed between the standard value and that obtained from the microfluidic disk.

C. Estimation of blood viscosity

Blood viscosity is greatly influenced by its hematocrit level. Since hematocrit basically indicates the proportion of the cellular material in the blood, a higher hematocrit value would naturally lead to a reduction in the fluidity or, conversely, an increment in the rigidity of the blood. This is manifested in the form of increased viscous resistance to deformation or, in other words, to the flow. Therefore, an increase in the hematocrit level of blood is directly manifested in an increase in the viscosity. The most commonly utilized empirical expressions for this dependence are given by the famous Power Law model,[95–97]

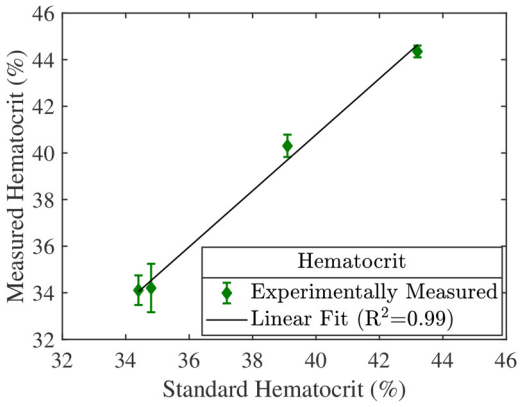

FIG. 4. Comparison of the blood hematocrit values obtained from our compact disc device (y axis) and the standard method (x axis). A high value of correlation ($R^2 = 0.99$) establishes the validity of the proposed method.

$$\tau = k(\dot{\gamma})^n, \tag{2}$$

$$k = c_1 \exp(c_2 \times Ht), \tag{3}$$

$$n = 1 - (c_3 \times Ht), \tag{4}$$

where τ is the shear stress, $\dot{\gamma}$ is the shear rate, k is the flow consistency index, n is the flow behavior index, $c_1 = 0.00148$, $c_2 = 0.0512$, $c_3 = 0.00499$, and Ht is the hematocrit of the blood. For estimation of blood viscosity, we focus our attention on the coefficients k and n. An apparent viscosity can be defined as

$$\mu_{app} = k(\dot{\gamma})^{n-1}, \tag{5}$$

i.e., for a given shear rate, the apparent viscosity will be determined by the power law indices (k, n). Since we have already determined the hematocrit level of blood in Sec. III B (Fig. 3), we can utilize that to determine the power law indices (k, n) by inserting the data in Eqs. (3) and (4). We have compared the estimated values of k, n with the rheological data (Fig. 5). An excellent agreement between the standard (from rheometer) and the estimated (from the compact disk) values of the indices establishes the validity of the proposed method to estimate blood viscosity. It may be observed that the flow consistency index as determined by the disk based hematocrit and empirical relation is slightly higher than that measured from the rheometer [Fig. 5(a)]. This is due to the fact that during the rheometer measurements, there is a slight sedimentation of the cellular material within the blood due to gravity. This may

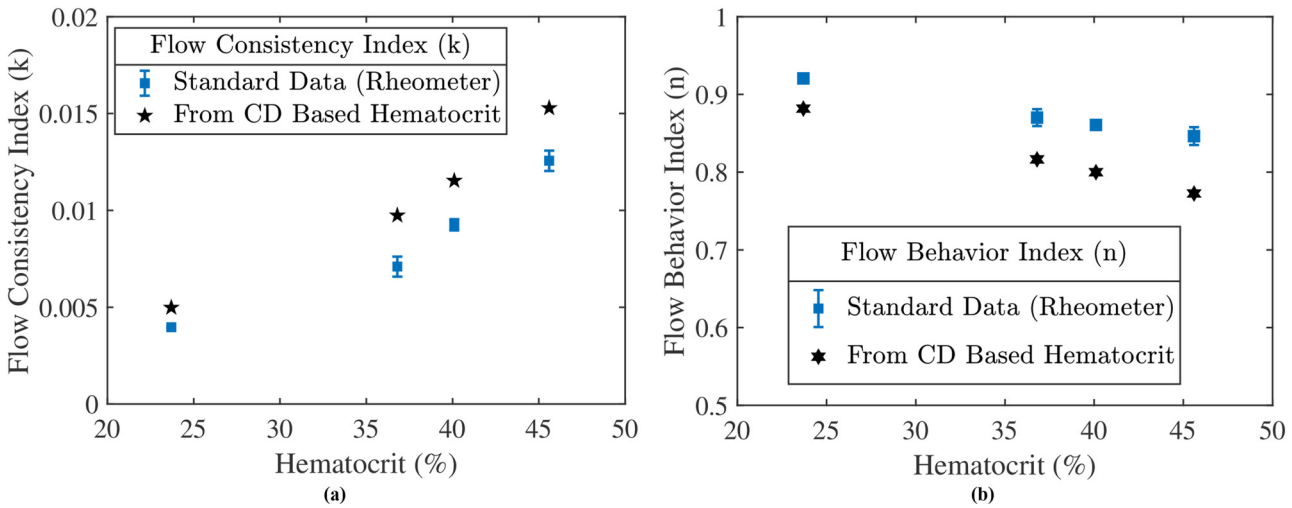

FIG. 5. Comparison of the power law indices for blood viscosity obtained from the compact disc device and the standard method at different hematocrit levels. Standard data here refer to the indices obtained from the viscosity-shear rate curve obtained from the rheometric measurements. It must be noted that there are no error bars associated with the CD based data as the mean value of the measured hematocrit has been utilized for estimating the indices with the aid of empirical relations. (a) Flow consistency index k; (b) flow behavior index n.

lead to an effectively decreased hematocrit in comparison to the true hematocrit (obtained by our device). This apparent decrease leads to a lower value of the flow consistency index [Eq. (3)] and a higher value of the flow behavior index [Eq. (4)] as measured by the rheometer. Note that once the power law indices are determined, the apparent viscosity can be determined as well at any given shear rate. Quite often, the Newtonian viscosity (when the fluid behaves like a Newtonian fluid at high shear rates) is of practical interest. That too can be determined from the power law indices with the aid of Eq. (5). In essence, once we determine the power law indices from the CD, we can then estimate the blood viscosity.

D. Erythrocyte sedimentation rate measurement

Erythrocyte sedimentation rate is a measure of the sedimentation of red blood cells with time in a given sample of whole blood. Due to the gravitational force, cellular components of blood especially RBCs settle toward the bottom, whereas the substrate like plasma appears at the top. In a rotating disk platform, we reassign the role of gravitational force to the centrifugal force. Its motivation lies in the fact that a centrifugal force field can be modulated by simply controlling the rotational speed of the platform and much greater sensitivity to the input parameter, i.e., rotational speed ($F_{cent} \sim \omega^2$) also acts as an encouragement. Due to this, the role of the gravitational field can be played by the centrifugal force field with a greater degree of flexibility, modulation, and in much lesser time, i.e., in minutes instead of hours.

For sedimentation in the traditional way, the gravitational effect and the viscous effect play crucial roles. The interplay between these two effects decides the ESR. The viscous effects are dictated by blood rheology, which, in turn, is strongly influenced by the hematocrit level. The gravitational force leads the transport of the RBCs (and the other constituents of the whole blood) toward the higher body force location (vertically downward, toward the surface of earth), whereas the hematocrit level decides the resistance that is to be offered to this transport. Therefore, the ESR depends on the flow rate as dictated by the body force and the viscous resistance as determined by the hematocrit level or simply the proportion of the RBCs in a given blood volume. This dependence may also be expressed as[98]

$$\mathrm{ESR} \sim (T^{-1})(1 - Ht)^2 10^{-1.82*Ht}. \tag{6}$$

In the above equation, T signifies the time in which a fixed volume of blood travels a given distance. Note that we have appropriated this equation for our method of ESR estimation. Conventionally, T would be replaced by an equivalent velocity term that would be indicative of velocity of the interface between the plasma and the RBCs. This interface velocity would be largely dictated by the proportion of RBCs or simply the hematocrit. Now, the flow of the whole blood is dictated by rheology, which, in turn, is strongly influenced by its hematocrit fraction. Hence, by means of the blood hematocrit level, there is an equivalence between the whole blood flow and the velocity of plasma-RBCs interface. We utilize this equivalence to replace the interface velocity term by the flow rate, which would be inversely related to the time taken (T) by a fixed volume of blood to be transported over a given distance. The time data measurement is done in the type (A) channel [Figs. 1(b) and 2(d)]. As already described in Sec. II D, a fixed amount of the blood sample is inserted in the loading reservoir of the type (A) channel, and under rotation at ω_{fl}, the time taken for the blood to completely fill the end reservoir is measured.

For a fixed set of operating conditions of channel geometry and rotational speed, the velocity will only be a function of the

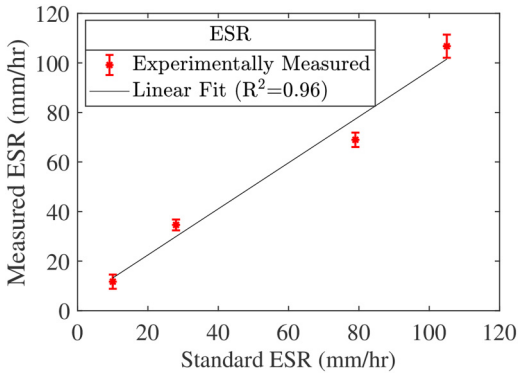

FIG. 6. Comparison of the ESR values obtained from the compact disc device (y axis) and the standard method (x axis). A high value of correlation ($R^2 = 0.96$) establishes the validity of the proposed method.

fluid (blood in this case) that is being transported through that channel. To address this, we estimate the range of linear velocity for a sample case of blood at 45% hematocrit level, at 1150 RPM (refer supplementary material for details on the estimation of velocity). The estimated range is found to be ≤ 1.2 mm/s. The maximum linear velocity and the maximum shear stress are found to be of the order of 1 mm/s and 10^{-1} Pa, respectively. These are rather low in magnitude. Hence, even on accounting for different blood compositions by means of different hematocrit levels, these values of linear velocity and shear stress may remain sufficiently low. Additionally, since the variables with regard to the local calibration of the device are the operating rotational speed ω_{fl} and the channel cross section, the absolute values of the linear velocity and associated shear stress are not expected to significantly affect the measurement unless there is a great deal of deviation from the proposed guidelines of device fabrication, operation, and measurement.

We now have both the parameters T and Ht to estimate the ESR [Eq. (6)]. The results obtained from Eq. (6) are scaled with the calibration equation as Measured ESR $= 5739^*((T^{-1})(1-Ht)^2 10^{-1.82^*Ht}) + 3.899$. The results, thus, obtained are depicted in Fig. 6. A high value of the linear correlation ($R^2 = 0.96$) establishes the validity of the proposed method and elicits excitement for its deployment as a POC device in resource-limited settings.

IV. CONCLUSIONS

In essence, we propose a novel portable spinning disk for rapid measurement of ESR, hematocrit, and blood viscosity. A simple experimental scheme with minimal sophistication is proposed that utilizes established empirical relations to estimate the aforementioned parameters. We have utilized the inherent centrifugal force present in any rotating environment for the actuation of device. The device operates at moderate rotational speeds that enforce lesser constraints on infrastructure quality. The measuring tool is a simple and most readily available standard 15 cm ruler, and the subsequent mathematical requirements hardly exceed the high school level. This opens up interesting avenues to look at this device as a potential candidate for point-of-care deployment in resource-limited settings without requiring any chemical analysis to measure some of the most significant blood parameters that influence infectious conditions in blood.

SUPPLEMENTARY MATERIAL

See the supplementary material for computational fluid dynamics (CFD) based analysis of the problem addressed in this work.

ACKNOWLEDGMENTS

The authors would like to acknowledge the financial support from MHRD and ICMR through IMPRINT grant (Sanction Letter No. F.No.:35-10/2016-TS-I). R.A. and S.P. acknowledge the supervision of Mr. Siddhartha Mukherjee of Microfluidics Laboratory for the rheological measurements. The authors also acknowledge the biological samples supplied by Mr. Rajib Das of BC Roy Hospital at IIT Kharagpur. S.C. acknowledges the financial support provided by DST, Government of India, through Sir J. C. Bose National Fellowship.

REFERENCES

[1]S. Zehnle, M. Rombach, R. Zengerle, F. von Stetten, and N. Paust, Biomicrofluidics **11**, 024114 (2017).
[2]Y. J. Kang, Y.-R. Ha, and S.-J. Lee, Biomicrofluidics **8**, 044114 (2014).
[3]C.-H. Shih, C.-H. Lu, J.-H. Wu, C.-H. Lin, J.-M. Wang, and C.-Y. Lin, Sens. Actuators B Chem. **161**, 1184 (2012).
[4]K. Wang, R. Liang, H. Chen, S. Lu, S. Jia, and W. Wang, Sens. Actuators B Chem. **251**, 242 (2017).
[5]A. A. Sayad, F. Ibrahim, S. M. Uddin, K. X. Pei, M. S. Mohktar, M. Madou, and K. L. Thong, Sens. Actuators B Chem. **227**, 600 (2016).
[6]A. Sayad, F. Ibrahim, S. Mukim Uddin, J. Cho, M. Madou, and K. L. Thong, Biosens. Bioelectron. **100**, 96 (2018).
[7]J.-W. Shangguan, Y. Liu, S. Wang, Y.-X. Hou, B.-Y. Xu, J.-J. Xu, and H.-Y. Chen, ACS Sens. **3**, 1416 (2018).
[8]S. Haeberle and R. Zengerle, Lab Chip **7**, 1094 (2007).
[9]H. J. Kim, C. Kwon, and H. Noh, ACS Sens. **4**, 9b01034 (2019).
[10]P. S. Khiabani, A. H. Soeriyadi, P. J. Reece, and J. J. Gooding, ACS Sen. **1**, 775 (2016).
[11]P. Yager, T. Edwards, E. Fu, K. Helton, K. Nelson, M. R. Tam, and B. H. Weigl, Nature **442**, 412 (2006).
[12]M. La, S. M. Park, and D. S. Kim, Biomicrofluidics **9**, 014104 (2015).
[13]N. Kolluri, C. M. Klapperich, and M. Cabodi, Lab Chip **18**, 75 (2018).
[14]S. Chakraborty and K. Tsuchiya, J. Appl. Phys. **103**, 114701 (2008).
[15]L. H. Nielsen, S. S. Keller, and A. Boisen, Lab Chip **18**, 2348 (2018).
[16]T. Oeschger, D. McCloskey, V. Kopparthy, A. Singh, and D. Erickson, Lab Chip **19**, 728 (2019).
[17]L. Gorgannezhad, M. Umer, M. N. Islam, N.-T. Nguyen, and M. J. A. Shiddiky, Lab Chip **18**, 1174 (2018).
[18]Y. J. Kang, Analyst **141**, 6583 (2016).
[19]K. Yamada, K. Suzuki, and D. Citterio, ACS Sens. **2**, 1247 (2017).
[20]J.-Y. Huang, H.-T. Lin, T.-H. Chen, C.-A. Chen, H.-T. Chang, and C.-F. Chen, ACS Sens. **3**, 174 (2018).
[21]A. Yakoh, S. Chaiyo, W. Siangproh, and O. Chailapakul, ACS Sens. **4**, 1211 (2019).
[22]A. Nilghaz, L. Guan, W. Tan, and W. Shen, ACS Sens. **1**, 1382 (2016).
[23]J. Heikenfeld, A. Jajack, J. Rogers, P. Gutruf, L. Tian, T. Pan, R. Li, M. Khine, J. Kim, J. Wang, and J. Kim, Lab Chip **18**, 217 (2018).

[24]E. E.-T. Hwu and A. Boisen, ACS Sens. **3**, 1222 (2018).
[25]M. Madou, J. Zoval, G. Jia, H. Kido, J. Kim, and N. Kim, Annu. Rev. Biomed. Eng. **8**, 601 (2006).
[26]O. Strohmeier, M. Keller, F. Schwemmer, S. Zehnle, D. Mark, F. von Stetten, R. Zengerle, and N. Paust, Chem. Soc. Rev. **44**, 6187 (2015).
[27]T. S. Kaminski, O. Scheler, and P. Garstecki, Lab Chip **16**, 2168 (2016).
[28]A. K. S. Lau, H. C. Shum, K. K. Y. Wong, and K. K. Tsia, Lab Chip **16**, 1743 (2016).
[29]A. Lenshof, M. Evander, T. Laurell, and J. Nilsson, Lab Chip **12**, 684 (2012).
[30]M. Rosenfeld, Rev. Sci. Instrum. **13**, 154 (1942).
[31]Y. Zhu, Y. Chen, and Y. Xu, Sens. Actuators B Chem. **276**, 313 (2018).
[32]S. Haeberle, T. Brenner, H.-P. Schlosser, R. Zengerle, and J. Ducrée, Chem. Eng. Technol. **28**, 613 (2005).
[33]S. Burger, M. Schulz, F. von Stetten, R. Zengerle, and N. Paust, Lab Chip **16**, 261 (2016).
[34]D. Chakraborty, M. Madou, and S. Chakraborty, Lab Chip **11**, 2823 (2011).
[35]D. Chakraborty and S. Chakraborty, Appl. Phys. Lett. **97**, 234103 (2010).
[36]S. Kar, S. Joshi, K. Chaudhary, T. K. Maiti, and S. Chakraborty, Appl. Phys. Lett. **107**, 244101 (2015).
[37]T. Brenner, T. Glatzel, R. Zengerle, and J. Ducrée, in *Proceedings of MTAS* (Royal Society of Chemistry, 2003), pp. 5–9.
[38]R. Agarwal, A. Sarkar, and S. Chakraborty, Analyst **144**, 3782 (2019).
[39]M. Grumann, A. Geipel, L. Riegger, R. Zengerle, and J. Ducrée, Lab Chip **5**, 560 (2005).
[40]F. Schwemmer, T. Hutzenlaub, D. Buselmeier, N. Paust, F. von Stetten, D. Mark, R. Zengerle, and D. Kosse, Lab Chip **15**, 3250 (2015).
[41]A. Kazemzadeh, A. Eriksson, M. Madou, and A. Russom, Nat. Commun. **10**, 189 (2019).
[42]S. Hugo, K. Land, M. Madou, and H. Kido, S. Afr. J. Sci. **110**, 1 (2014).
[43]J. Ducrée, S. Haeberle, S. Lutz, S. Pausch, F. von Stetten, and R. Zengerle, J. Micromech. Microeng. **17**, S103 (2007).
[44]R. Gorkin, J.-M. J. Park, J. Siegrist, M. Amasia, B. S. Lee, J.-M. J. Park, J. Kim, H. Kim, M. Madou, and Y.-K. Cho, Lab Chip **10**, 1758 (2010).
[45]S. Hosseini, M. M. Aeinehvand, S. M. Uddin, A. Benzina, H. A. Rothan, R. Yusof, L. H. Koole, M. J. Madou, I. Djordjevic, and F. Ibrahim, Sci. Rep. **5**, 16485 (2015).
[46]T.-H. Kim, H. Hwang, R. Gorkin, M. Madou, and Y.-K. Cho, Sens. Actuators B Chem. **178**, 648 (2013).
[47]M. Amasia and M. Madou, Bioanalysis **2**, 1701 (2010).
[48]R. Uddin, M. Donolato, E.-T. Hwu, M. F. Hansen, and A. Boisen, Sens. Actuators B Chem. **272**, 634 (2018).
[49]J. Steigert, M. Grumann, T. Brenner, L. Riegger, J. Harter, R. Zengerle, and J. Ducrée, Lab Chip **6**, 1040 (2006).
[50]E. Mahmodi Arjmand, M. Saadatmand, M. R. Bakhtiari, and M. Eghbal, Talanta **190**, 134 (2018).
[51]S. Kar, T. K. Maiti, and S. Chakraborty, Analyst **140**, 6473 (2015).
[52]S. Kar, U. Ghosh, T. K. Maiti, and S. Chakraborty, Lab Chip **15**, 4571 (2015).
[53]S. Chien, S. Usami, H. M. Taylor, J. L. Lundberg, and M. I. Gregersen, J. Appl. Physiol. **21**, 81 (1966).
[54]B. L. Walton, M. Lehmann, T. Skorczewski, L. A. Holle, J. D. Beckman, J. A. Cribb, M. J. Mooberry, A. R. Wufsus, B. C. Cooley, J. W. Homeister, R. Pawlinski, M. R. Falvo, N. S. Key, A. L. Fogelson, K. B. Neeves, and A. S. Wolberg, Blood **129**, 2537 (2017).
[55]T. L. Fabry, Blood **70**, 1572 (1987).
[56]C.-H. Cha, C.-J. Park, Y. J. Cha, H. K. Kim, D. H. Kim, Honghoon, J. H. Bae, J.-S. Jung, S. Jang, H.-S. Chi, D. S. Lee, and H.-I. Cho, Am. J. Clin. Pathol. **131**, 189 (2009).
[57]N. V. Greidanus, J. Bone Jt. Surg. **89**, 1409 (2007).
[58]M. B. Andresdottir, Am. J. Epidemiol. **158**, 844 (2003).
[59]N. R. Broek and E. A. Letsky, BJOG **108**, 1164 (2001).
[60]M. Plebani, S. De Toni, M. C. Sanzari, D. Bernardi, and E. Stockreiter, Am. J. Clin. Pathol. **110**, 334 (1998).
[61]X. Xu, L. Yu, and Z. Chen, Ann. Biomed. Eng. **38**, 3210 (2010).
[62]J. Zhang, P. C. Johnson, and A. S. Popel, Microvasc. Res. **77**, 265 (2009).
[63]T.-X. Zhao and B. Jacobson, Med. Biol. Eng. Comput. **35**, 181 (1997).
[64]D. Gilmour and A. J. Sykes, Br. Med. J. **2**, 1496 (1951).
[65]K. Cha, E. F. Brown, and D. W. Wilmore, Physiol. Meas. **15**, 499 (1994).
[66]A. Yoshikoshi, A. Sakanishi, and Y. Toyama, Rev. Sci. Instrum. **75**, 4379 (2004).
[67]Y. Kang and B. Kim, Micromachines **9**, 318 (2018).
[68]G. A. M. Pop, D. J. Duncker, M. Gardien, P. Vranckx, S. Versluis, D. Hasan, and C. J. Slager, Neth. Heart J. **10**, 512–516 (2002).
[69]R. Rosencranz and S. A. Bogen, Pathol. Patterns Rev. **125**, S78 (2006).
[70]G. A. M. Pop, L. L. A. Bisschops, B. Iliev, P. C. Struijk, J. G. van der Hoeven, and C. W. E. Hoedemaekers, Biosens. Bioelectron. **41**, 595 (2013).
[71]Y. Jun Kang, J. Ryu, and S.-J. Lee, Biomicrofluidics **7**, 044106 (2013).
[72]B. J. Kim, Y. S. Lee, A. Zhbanov, and S. Yang, Analyst **144**, 3144 (2019).
[73]Y. J. Kang, Biomicrofluidics **12**, 024116 (2018).
[74]Y. J. Kang, Analyst **144**, 3556 (2019).
[75]Y. Jun Kang, E. Yeom, and S.-J. Lee, Biomicrofluidics **7**, 054111 (2013).
[76]Y. Kang, Micromachines **9**, 467 (2018).
[77]A. W. Browne, L. Ramasamy, T. P. Cripe, and C. H. Ahn, Lab Chip **11**, 2440 (2011).
[78]Z. Isiksacan, O. Erel, and C. Elbuken, Lab Chip **16**, 4682 (2016).
[79]Y. J. Kang, Anal. Methods **10**, 1805 (2018).
[80]E. Yeom and S. J. Lee, Biomicrofluidics **9**, 024110 (2015).
[81]R. P. Kate, P. K. Das, and S. Chakraborty, J. Fluid Mech. **573**, 247 (2007).
[82]S. Chakraborty and S. K. Som, Int. J. Heat Mass Tran. **48**(13), 2801 (2005).
[83]S. Das, T. Das, and S. Chakraborty, Sens. Actuators B Chem. **114**, 957 (2006).
[84]A. Bandopadhay, D. Tripathi, and S. Chakraborty, Phys. Fluids **28**, 052002 (2016).
[85]S. Das, S. Chakraborty, and S. K. Mitra, Phys. Rev. E **85**, 051508 (2012).
[86]S. Chakraborty and S. Ray, Phys. Fluids **20**, 083602 (2008).
[87]S. Das and S. Chakraborty, AIChE J. **53**, 1086–1099 (2007).
[88]A. Garai and S. Chakraborty, Electrophoresis **31**, 843–849 (2010).
[89]S. P. Das, S. Chakraborty, and P. Dutta, Heat Transfer Eng. **25**, 54 (2004).
[90]S. Chakraborty, Appl. Phys. Lett. **90**, 034108 (2007).
[91]S. Sarkar, P. M. Raj, S. Chakraborty, and P. Dutta, Numer. Heat Transfer A **42**, 307 (2002).
[92]P. M. Raj, S. Sarkar, S. Chakraborty, G. Phanikumar, and P. Dutta, Int. J. Heat Fluid Flow **23**, 298 (2002).
[93]S. Kar, M. Dash, T. K. Maiti, and S. Chakraborty, Analyst **140**, 1432 (2015).
[94]L. Riegger, M. Grumann, J. Steigert, S. Lutz, C. P. Steinert, C. Mueller, J. Viertel, O. Prucker, J. Rühe, R. Zengerle, and J. Ducrée, Biomed. Microdevices **9**, 795 (2007).
[95]F. J. Walburn and D. J. Schneck, Biorheology **13**, 201 (1976).
[96]S. Chakraborty, Lab Chip **5**, 421 (2005).
[97]S. Chakraborty, Anal. Chim. Acta **605**, 175 (2007).
[98]M. A. McGrath, Pathology **19**, 112 (1987).